

# Petrological characterisation of the “Tertiary quartzites” from the site of Troisdorf-Ravensberg (North Rhine-Westphalia, Germany): first insights in Middle Palaeolithic outcrop exploitation

*Petrologische Charakterisierung der „tertiären Quarzite“ von Troisdorf-Ravensberg (Nordrhein-Westfalen, Deutschland): Erste Einblicke in die Nutzung des mittelpaläolithischen Aufschlusses*

Alejandro PRIETO<sup>1,2\*</sup>, Iñaki YUSTA<sup>3</sup>, Andreas PASTOORS<sup>1</sup> & Erich CLAßEN<sup>4</sup>

<sup>1</sup> Institut für Ur- und Frühgeschichte, Friedrich-Alexander-Universität, Erlangen-Nürnberg, 91054 Erlangen, Germany; email: alejandro.prieto@ehu.eus

<sup>2</sup> Department of Geography, Prehistory and Archaeology, University of the Basque Country (UPV/EHU), Paseo de la Universidad, 5., 01006 Vitoria-Gasteiz, Spain

<sup>3</sup> Department of Mineralogy and Petrology, University of the Basque Country (UPV/EHU) Apdo.664, 48080, Bilbao, Spain

<sup>4</sup> LVR-State Service for Archaeological Heritage, Endenicher Str. 133, 53115 Bonn, Germany

**ABSTRACT** - The new excavations carried out at the site of Troisdorf-Ravensberg in 2015 have brought to light an essential part of Neanderthal daily life: the procurement mechanism of lithic raw material. The first hypothesis to understand this site propounds that it was used as a quartzite workshop or a quarry site where extractive and first knapping activities were performed in the Middle Palaeolithic. Against this background this study focusses on the petrological characterisation of the quartzites from Troisdorf-Ravensberg using a solid geoarchaeological protocol based on petrographic-stereomicroscopic petrology and geochemical composition. These procedures allowed us to characterise the “Tertiary quartzites” at this site and to establish two types and two varieties of this raw material based on the features which led us to understand the stone formative processes. The latter is related with sedimentary processes and the formation of silcretes. Preliminary data puts forward a selective extraction and exploitation of a specific facies, the secondary exploitation of a by-product type, and the discard of the last variety. This complex raw material exploitation is suggested by the technological markers observed, which connect the physical properties of the stone, based on silica cementation of the former quartz arenite, and the procurement strategies carried out by the Middle Palaeolithic people. The qualitative differences in the raw material are an important aspect of the anthropogenic selection that can be identified in the Troisdorf assemblage. Other selection criteria, especially the morphology of the raw pieces or technological requirements, certainly play also a major role, but are not part of this contribution.

**ZUSAMMENFASSUNG** - Die neuen Ausgrabungen, die 2015 in Troisdorf-Ravensberg durchgeführt werden, bringen einen wichtigen Teil des Neandertaler-Alltags ans Licht: den Beschaffungsmechanismus von lithischem Rohmaterial. Die erste Interpretation der Funktion der mittelpaläolithischen Fundstelle zieht eine Quarzit-Werkstatt oder einen Steinbruch in Betracht, in dem der Abbau und erste Arbeiten der Steinschläger durchgeführt wurden. Vor diesem Hintergrund fokussiert die vorliegende Untersuchung auf die petrologische Charakterisierung anhand eines soliden geoarchäologischen Protokolls, das auf petrographisch-stereomikroskopischer Petrologie und geochemischer Zusammensetzung der vorgefundenen Gesteine basiert. Diese Verfahren ermöglichen es, die „tertiären Quarzite“ aus Troisdorf-Ravensberg zu charakterisieren und sowohl zwei Typen als auch zwei Varietäten dieses Materials zu bestimmen, die mit ihren Entstehungsprozessen in Zusammenhang stehen. Letzteres hängt mit den sedimentären Prozessen und der Bildung von Silcreten zusammen.

Die Ergebnisse der Analyse zeigen, dass in Troisdorf-Ravensberg das verfügbare Rohmaterial unterschiedlich gehandhabt wurde: die selektive Gewinnung und Nutzung einer bestimmten Fazies, die weniger bedeutsame Verwendung eines Nebenprodukttyps und die Auslassung der letzten Varietät. Diese komplexe Nutzung des Rohmaterials wird durch die beobachteten technologischen Marker unterstützt, die die physikalischen Eigenschaften des Gesteins, basierend auf der Siliciumdioxid-Zementierung des ehemaligen Quarzarenits, und die Beschaffungsstrategien der mittelpaläolithischen Jäger und Sammler verbinden. Die qualitativen Unterschiede im Rohmaterial sind ein wichtiger Aspekt der in der Troisdorfer Sammlung fassbaren anthropogenen Auswahl. Weitere Auswahlkriterien, vor allem die Morphologie der Rohstücke oder technologische Anforderungen, spielen sicherlich auch eine große Rolle, sind aber nicht Bestandteil dieses Beitrags.

\*corresponding author

**KEYWORDS** - Middle Palaeolithic, raw material, silcrete, geoarchaeology, petrography, Wavelength Dispersive-X Ray Fluorescence  
*Mittelpaläolithikum, Rohmaterial, Silcrete, Geoarchäologie, Petrographie, Wellenlängen-Dispersions-Röntgenfluoreszenz*

## Introduction

Lithic procurement during the Palaeolithic was a time consuming task which required specific behavioural and practical operations to be performed, as discussed by several authors (e.g. Bamforth 2006; Binford 1979; Gould 1978; Vaquero & Romagnoli 2017). Direct procurement, instead of embedded or neutral procurement models, is mandatory to take advantage of environments where appropriate lithic resources are scarce (Brantingham 2003). Although lithic procurement could be included in other economic activities, specific actions are required to obtain raw material in places where suitable and desirable raw material is restricted to small areas, in small proportions or/and specific stratum or veins.

Human mobility, transportation of raw material and spatial management of the environment are the three basic strategies to acquire raw material restricted to few areas, as observed in several Middle Palaeolithic sites in Europe (e.g. Doronicheva & Shackley 2014; Gómez de Soler et al. 2019; Turq et al. 2013; Turq et al. 2017). The selection of determinate stones in areas in which raw material was disperse and scarce, was also a basic mechanism used by Middle Palaeolithic people. Moreover, these kinds of behaviours are not often mentioned in scientific literature (i.e. Daffara et al. 2019; Fernandes et al. 2008; Roy et al. 2017). Finally, selective extraction or even Palaeolithic quarrying processes of a specific type or variety of raw material were the last procurement strategies used by Middle Palaeolithic groups to take advantage of particular environments and landscapes, as proposed by several authors (e.g. Baena et al. 2011; Finkel et al. 2019; Gopher & Barkai 2014; Groucutt et al. 2017).

The research presented here aims to understand the physical properties of the lithologies knapped by Palaeolithic people as an important aspect to understand the raw material procurement strategies carried out by the humans who inhabited the Middle-Lower Rhine Valley (Germany). This is done by analysing the quartzite assemblage from Troisdorf-Ravensberg obtained during recent excavations in 2015 (Pastoors et al. 2016). Troisdorf-Ravensberg is an open-air site in the northeast of the city of Troisdorf (North Rhine Westphalia), close to the confluence of the Agger and Sieg rivers on the south-eastern border of the Lower Rhine Embayment (*Niederrheinische Bucht*). It is on the slope of Ravensberg, which is the highest elevation (123 metres a.s.l.) at the southern border of the Wahner Heide, a natural landscape on the middle

terrace of the Rhine (Fig. 1). From the geological standpoint, the archaeological site is situated in the so-called "*Köln Schichten*" (Köln Formation), a Tertiary (Late Oligocene-Early Miocene) cyclic fan of coastal deposits of interfingered marine and fluvial siliciclastic sands and white sediments very rich in quartz (Winterscheid & Kvaček 2016). Lignite, volcanic tuff, and locally silicified sand lenses ("Tertiary quartzites") are also documented in small proportions inside the latter formation (Skupin & Wold 2011; Udluft & Pfeffer 1977; Zitzmann et al. 2002). This formation is partially covered by fine to medium sands transported by the wind during the Quaternary.

The assemblage recovered during the 2015 excavation is formed by 5 392 lithic pieces. Bones are not preserved. Only 418 pieces were identifiable as artefacts using formal and standard categories. The other stones selected during the excavation are blocks, frost sherds and pebbles. The main raw material is quartzite (>98% of the total pieces). Reduction strategies are varied, with recurrent (unidirectional and centripetal), preferential, discoidal, Kombewa and irregular/opportunistic methods. Numerical data is not available, but preliminary technological and typological considerations proposed a late Middle-Palaeolithic chronology for this site. Since the first excavation, undertaken in 1967 by G. Bosinski, this site was considered as a workshop in the immediate neighbourhood of the raw material outcrop (Fiedler & Veil 1974). In Troisdorf-Ravensberg, the technological characterisation, the distribution of finds and the stratigraphy of the 2015 excavation, also support the idea that the site was used as a workshop or even a quarry by Middle Palaeolithic populations (Pastoors et al. 2016). A quarry is considered here as a place used for extractive activities in recurrent and/or massive terms (Bamforth 2006; Gopher & Barkai 2014; Van Peer et al. 2010; Wragg Sykes et al. 2017).

In this research, the quartzites at this site were characterised for a better understanding of a part of the procurement mechanisms carried out by humans in the Middle Palaeolithic. A solid geoarchaeological procedure was based on petrographic-stereomicroscopic petrology and geochemical composition (Prieto et al. 2019, 2020). The use of these procedures enabled the characterisation of the quartzites from this site and the establishment of two types and two varieties based on the features which define the stone formation processes. Unfortunately, it was only possible to suggest hypothesis about the procurement using a non-numerical and qualitative technological



Fig. 1. Troisdorf-Ravensberg archaeological site in the 1:200 000 geological map (Zitzmann et al. 2002).

Abb. 1. Lage der archäologischen Fundstelle Troisdorf-Ravensberg. Die wichtigsten chrono-lithologischen Schichten sind auf Grundlage der geologischen Karte 1:200.000 wiedergegeben (Zitzmann et al. 2002).

characterisation. Therefore, the conclusions reached must be nuanced and contrasted with future numerical characterisations. For the understanding of the complete procurement mechanisms it is necessary to link the obtained results of the characterisation of the quartzites with other selection criteria, especially the morphology of the raw pieces or technological requirements. However, this is not yet possible at this stage of the investigations. Therefore, only first non-numerical and qualitative impressions can be listed here. A study with reliable data will be explored in follow-up research.

It should be noted that, despite being the second most-often used lithic raw material in the European Palaeolithic, quartzite has not been studied as much as flint or obsidian (Prieto 2018). This situation creates a lack of information and bias in understanding the catchment strategies pursued by prehistoric societies in: a) regions where flint is not predominant; in b) a chronological framework in which quartzite is relevant,

such as the Lower and Middle Palaeolithic; and in c) catchment strategies unrelated with raw material transportation, which mainly promote historical narratives based on human mobility (Prieto 2020). Nevertheless, in recent years quartzite from archaeological deposits has been studied from geoarchaeological perspectives by combining different destructive methodologies such as petrographic analysis and geochemical procedures (Blomme et al. 2012; Cnudde et al. 2013; Dalpra & Pitblado 2016; Pedergrana, 2017; Pitblado et al. 2012; Prieto et al. 2019; Prieto et al. 2020; Roy et al. 2017; Soto et al. 2020; Veldeman et al. 2012). These studies reflect the ambiguity of the term quartzite in archaeological literature, where it can refer to different geological origins, from clearly metamorphic to sedimentary. Similar discrepancies between megascopic identification and laboratory analysis are also mentioned by petrologists, especially when quartzite is used as a field name (Howard 2005; Skolnick 1965).

## Materials and Methods

The materials studied here derived from the assemblage recovered in the recent excavation in Troisdorf-Ravensberg (Pastoors et al. 2016). The initial sampling process used appearance to the naked eye and hand-magnifiers to obtain the most representative groups of quartzite. 60 pieces were selected for the non-destructive analysis. Besides homogeneous samples, we could differentiate pieces with multiples facies. A total of 11 pieces have two different surfaces and another 14 have three surfaces. All of them were analysed using non-destructive stereomicroscopy. Finally, we selected the ten most representative items (Fig. 2) for analysis using petrography and Wavelength Dispersive-X Ray Fluorescence analysis (WDXRF). From these ten samples, six have just one facies, two have two different facies and a further two samples have three facies. Each of these facies was considered as a different sample or unit of study.

The methodology is based on a multi-scalar approach that combines naked-eye descriptions, stereomicroscopic surface characterisation at different magnification (10-20x, 50x, and 250x magnification), thin section description and WDXRF analysis. The thin section characterisation was based on the proposal made by Prieto et al. (2019). All thin sections were produced and analysed at the Laboratory of Sample Preparation, Department of Mineralogy and Petrology, University of the Basque Country-UPV/EHU, Spain. They were analysed using a Nikon Eclipse LV100N POL microscope. Photographs were taking using the Nikon D90 camera adapted to the microscope.

We characterised the texture, distinguishing between a) clastic texture with matrix or cement, b) clastic grained texture, and c) mortar texture. The packing of each section was characterised as a) floating, b) punctual, c) tangential, d) complete, or e) saturated. The characterisation of quartz grains uses the following criteria a) detrital quartz grain, b) grains with concave-convex boundaries, c) undulose extinction on thin-section quartzite, d) regrowth of quartz syntaxial cement e) stylolites or serrated boundaries, f) Böhm lamellae, and (f) recrystallized grains. Their frequency was quantified as a) very abundant, when the grain type amounts to over 50 % of the total in the sample, b) major, with a presence between 5 % and 50 %, and c) minor (or trace) if less than 5 % of the studied quartz grains.

Metrical characterisation of size, shape and orientation of quartz grains was done by digital image processing of representative sectors of thin sections. The measurements obtained are a) size of the particle, using the secondary axis, b) circularity index, a measurement that describe the irregularity of each particle using a number between 0 and 1, c) roundness index, a measurement that describes the elongation of each particle using a number between 0 and 1, and d) angle of each particle to analyse preferential

orientation of quartz grains in each sample using Rayleigh's R-test (Davis 1986; Mardia 1975).

Finally, we described the matrix and cement according to their mineral composition. Here we mainly described clayey and siliceous matrix and microcrystalline quartz cement (Fig. 3). Quantification of both categories was done according to the following criteria a) very abundant, when matrix or cement type amounts to over 20 % of the total in the sample, b) major, with a presence between 20 and 5 % in the sample, and c) minor (or trace) if less than 5 % of the total in the sample. Finally, we characterised the presence of non-quartz minerals in thin sections.

The semiquantitative chemical composition of the lithics was determined by WDXRF using a PANalytical Axios Advanced PW4400 XRF spectrometer (4kW Rh anode SST-mAX X-ray tube) at the SGIker Facilities (UPV/EHU). After being cut for thin sections, the ten fresh surfaces were directly placed in 20 mm-diameter sample holders. They were measured with 3 kW excitation power using PANalytical's Omnia stand-alone analysis software. The analysed sections were  $\approx 300 \text{ mm}^2$ , except for some very small debitage pieces ( $100 \text{ mm}^2$ ). One measurement was taken for each sample without taking into account the different facies. We also applied XRF quantitative analysis ( $n=7$  samples) using fused beads prepared after mixing 0.2 g of finely ground sample with 3.8 g of a lithium borate flux (Spectromelt A12, Merck) and LiBr as non-wetting agent. The samples analyzed were made on one of each facies of Tr-222-12 (3), one of each facies of Tr-128-5, and the single-facies samples Tr-1-18 and Tr-161-2-3. These measurements allowed us to test the first measurements and to understand the chemical composition of different facies in the same sample.

Stereoscopic characterisation followed the protocol established by Prieto et al. (2020), while taking into account specific features of these quartzites. These new features are related to the presence of cement and/or matrix. They are the mineralogical and textural description of the type of matrix or cement and their quantification. The latter used the criteria applied to the thin sections, that is a) very abundant; b) major; and c) minor (or trace). The types of matrix and cement are also related to those observed in the thin sections. Therefore, there are clayey or siliceous matrix and microcrystalline quartz cement (Fig. 3). These criteria are added to those described in a well-founded methodology, such as texture, packing or quartz grain features, qualitative characterisation of quartz grain size and orientation, and finally, qualitative characterisation of non-quartz mineral.

## Results

### Thin section characterisation and geochemical composition

Figure 4 summarises texture, packing and quartz grain feature characterisation differentiating each facies in

each sample, and finally grouped by them. A total of 16 facies were analysed. Figure 5 reviews matrix, cement, and non-quartz mineral identification using the same grouping criteria. All in all, petrographic characterisation reveals the presence of two different

petrogenetic types. The matrix or cemented quartz arenite (MA type) is the more frequent type, while the syntaxially overgrown orthoquartzite (OO type) is less common. Based on the presence of cement and/or matrix, there are two different varieties within the first

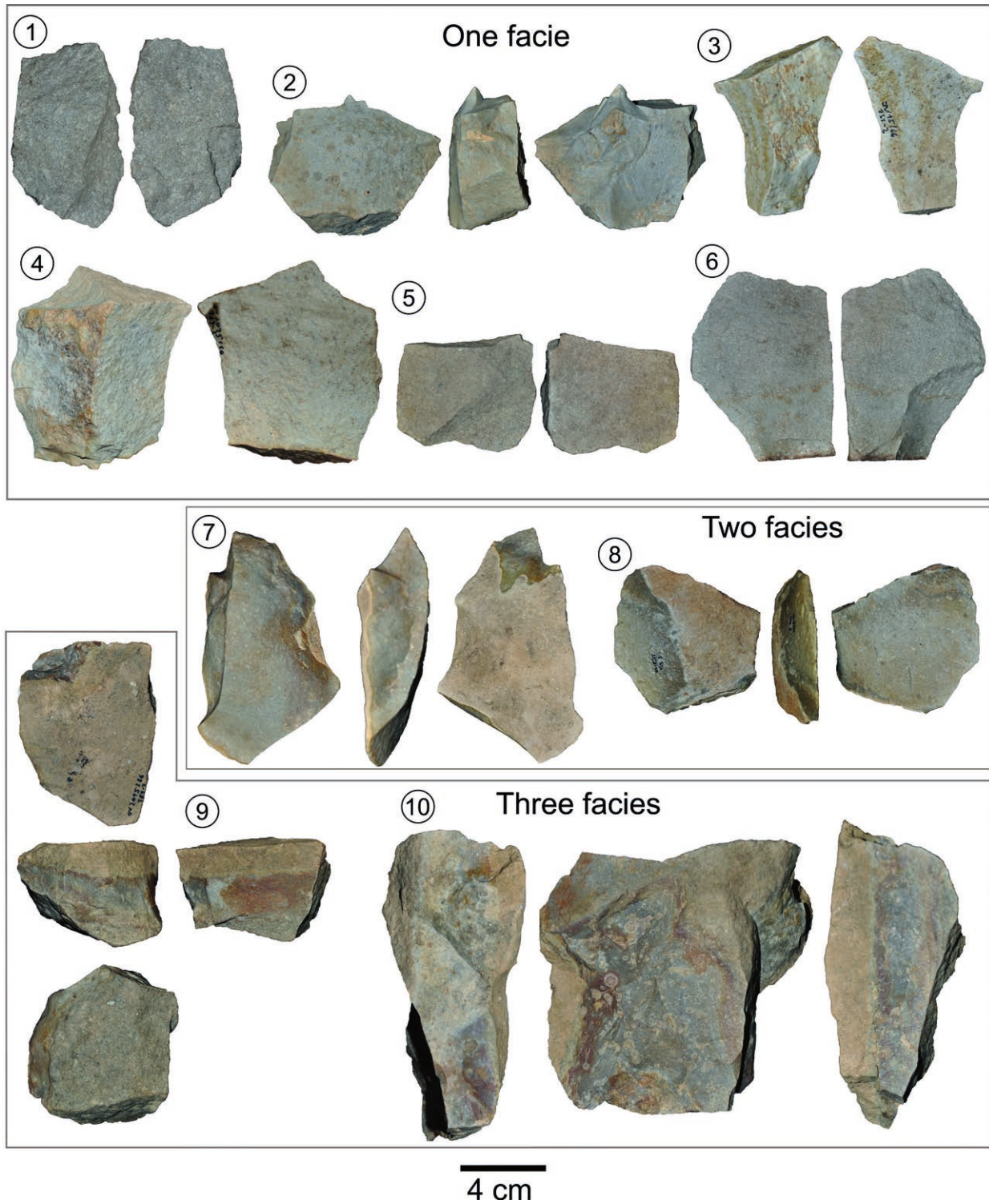


**Fig. 2.** Troisdorf-Ravensberg samples for petrography and chemical analysis. They are grouped according to the quantity of facies represented in each. 1) Tr-1-18; 2) Tr-223-3-2; 3) Tr-161-2-3; 4) Tr-161-2b-6; 5) Tr-129-2-4; 6) Tr-1-33; 7) Tr-254-2-1; 8) Tr-128-5; 9) Tr-161 2b-2; 10) Tr-222-12.

**Abb. 2.** Petrographie und chemische Analyse der Proben aus Troisdorf-Ravensberg. Gruppierung nach der Menge der jeweils dargestellten Fazies. 1) Tr-1-18; 2) Tr-223-3-2; 3) Tr-161-2-3; 4) Tr-161-2b-6; 5) Tr-129-2-4; 6) Tr-1-33; 7) Tr-254-2-1; 8) Tr-128-5; 9) Tr-161-2b-2; 10) Tr-222-12.

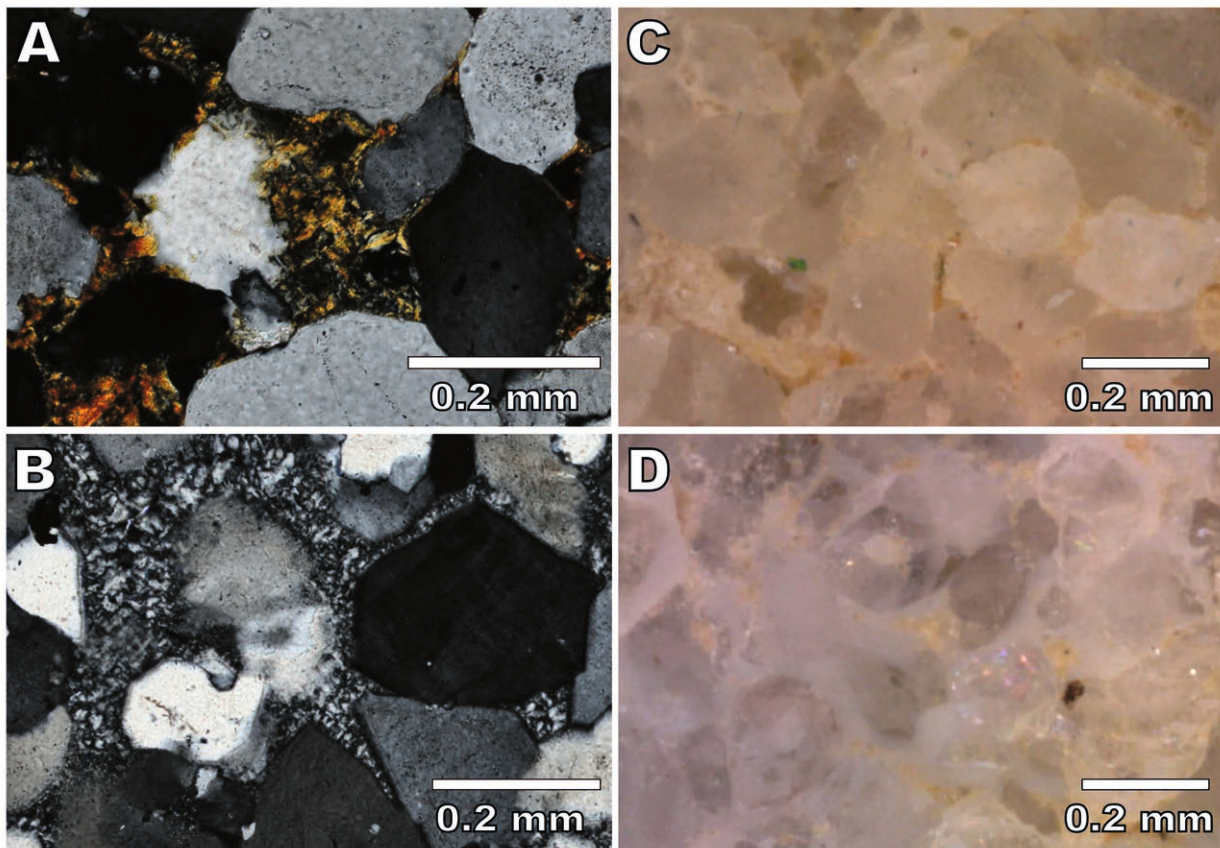


**Fig. 3.** Most representative matrix and cement described in the quartzite artefacts from Troisdorf-Ravensberg. A) Thin section detail at 200x magnification of clayey matrix of sample Tr-254-2\_f1. B) Thin section detail at 200x magnification of microcrystalline quartz cement of sample Tr-161-2b-6. C) Photomicrograph of the surface of Tr-254-2\_f1 in which it is possible to distinguish a reddish-brown matrix in between grains. They are more concentrated in some zones, showing variable reliefs. D) Photomicrograph of the surface of Tr-161-2b\_6 in which it is possible to distinguish white microcrystalline cement joining different quartz grains. The reliefs are gentle and grains are surrounded by a whitish halo.

**Abb. 3.** Repräsentativste Matrix und Zement, die in den Quarzit-Artefakten aus Troisdorf-Ravensberg beschrieben sind. A) Dünnschliff-Detail bei 200-facher Vergrößerung der tonigen Matrix der Probe Tr-254-2\_f1. B) Dünnschliff-Detail bei 200-facher Vergrößerung des mikrokristallinen Quarzzements der Probe Tr-161-2b-6. C) Mikroskopische Aufnahme der Oberfläche von Tr-254-2\_f1, in der eine rötlich-braune Matrix zwischen den Körnern sichtbar ist. Sie sind in einigen Zonen stärker konzentriert und zeigen variable Reliefs. D) Mikrofotografie der Oberfläche von Tr-161-2b\_6, in der man weißen mikrokristallinen Zement erkennen kann, der verschiedene Quarzkörner verbindet. Die Reliefs sind flach und die Körner sind von einem weißlichen Halo umgeben.

type. The first and most abundant cement is formed of microcrystalline quartz. This variety is named here as cemented quartz arenite with microcrystalline quartz (MA\_MQC). In contrast, in the other variety cement is almost completely absent and the matrix consists mainly of clayey minerals. The latter generally does not completely fill the main grain framework. We refer to this variety as clayey matrix quartz arenite (MA\_CM).

Metric characterisation of quartz grains shows a general heterogeneous distribution of quartz grains although most of them are situated between the very fine sand and fine sand categories (Fig. 6: A). Quartz grains range from the very fine silt and coarse silt categories, in which the presence of these two sizes are very small, to medium sand grains. There are no differences between quartz grain sizes depending on their petrogenetic types or varieties. All three varieties present similar curve descriptions and the differences in the percentages are simply caused by

the quantity of thin section analysed. The same conclusions are reached using the morphology of particle distribution in the three proposed types and varieties, as showed in Figure 6: B. Circularity and Roundness indexes are mainly higher than 0.5. These data point to regular outlines and non-elongated shapes. Partial differences between varieties are observable taking into account preferential orientation of particles in each section, as indicated by the examples showed on Figure 6: C.

X-Ray Fluorescence data reveal that  $\text{SiO}_2$  is the predominant component, with a mean value of 98.7 wt % and always >96 wt % (Fig. 7). Other components, such as  $\text{Al}_2\text{O}_3$ ,  $\text{Fe}_2\text{O}_3$  and  $\text{TiO}_2$  are represented in very small percentages, always <0.5 wt %. Occasionally, traces of  $\text{MgO}$ ,  $\text{CaO}$ ,  $\text{Na}_2\text{O}$  or  $\text{P}_2\text{O}_5$  are found only in some samples, while in the others they are below the detection limits of the method. No clear chemical differences are found between the different types or varieties identified by petrographic methods, due to

Sample	Packing	Texture	Quartz grain features					Petrogenetic Type
			Clastic quartz grain	Undlt. extinction quartz grain	Synt. ovgrowth quartz grain	Concv-con- vex q. grain limits	Saturated quartz grain	
Tr-161-2b-2_f1	Tangential	C&M/C	XX	-	XX	XXX	-	MA
Tr-222-12_f3	Tangential	C&M/C	XXX	XX	XX	-	-	MA
Tr-128-5_f1	Tangential	C&M/C	XXX	-	XX	XXX	-	MA
Tr-254-2_f1	Tangential	C&M/C	XXX	-	-	-	-	MA
Tr-1-33	Tangential	C&M/C	XXX	-	XX	-	-	MA
Tr-128-5_f2	Tangential	C&M/C	XXX	-	XX	XXX	-	MA
Tr-161-2-3	Punctual	C&M/C	XXX	-	X	-	X	MA
Tr-161-2b-2_f2	Punctual	C&M/C	XXX	XX	XX	-	-	MA
Tr-161-2b-6	Tangential	C&M/C	XXX	-	XX	XX	-	MA
Tr-222-12_f2	Tangential	C&M/C	XXX	-	XX	XX	-	MA
Tr-223-3-2	Tangential	C&M/C	XXX	-	X	-	-	MA
Tr-254-2_f2	Punctual	C&M/C	XXX	-	X	-	X	MA
Tr-1-18	Complete	CG	XX	-	XXX	XXX	-	OO
Tr-129-2-4	Complete	CG	X	-	XXX	XXX	-	OO
Tr-161-2b-2_f3	Complete	CG	XXX	XX	XX	-	-	OO
Tr-222-12_f1	Complete	CG	XX	-	XX	XXX	-	OO

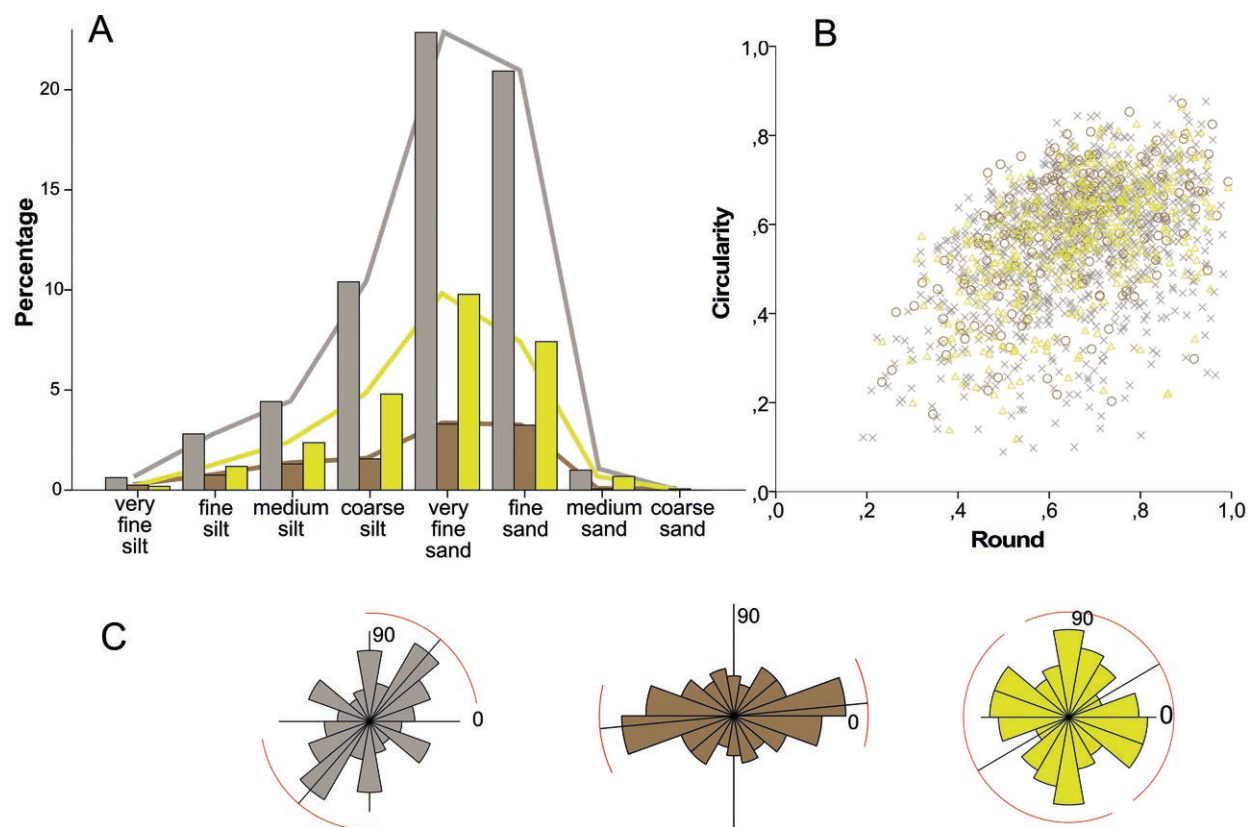
Fig. 4. Texture, packing and quartz grain features described in thin section samples differentiated by facies (denoted as f1, f2, f3). Petrogenetic type is also showed. Rock texture is simplified as C&M/C for clastic texture with matrix or cement and CG for clastic grained texture. Quartz grain feature presence is scaled as X, for minor or trace presence; XX, for major presence; and XXX for very abundant.

Abb. 4. Textur-, Füllkörper- und Quarzkornmerkmale, beschrieben in Dünnschliffproben, die nach Fazies (bezeichnet als f1, f2, f3) unterschieden werden. Auch der petrogenetische Typ wird gezeigt. Die Gesteinstextur wird vereinfacht als C&M/C für klastische Textur mit Matrix oder Zement und CG für klastische körnige Textur bezeichnet. Das Vorhandensein von Quarzkornmerkmalen wird mit X für geringe oder einfache Anwesenheit, mit XX für starke und mit XXX für sehr starke Präsenz skaliert.

Sample	Matrix		Cement		Mineral identified							Petrogen. Type + Mineral variety
	Type	%	Type	%	Zircon	Rutile	Mica	Chlorite	Clay	Pyrite	Fe-oxides	
Tr-161-2b-2_f1	Clay	XX	-	-	-	-	-	-	-	-	X	MA_CM
Tr-222-12_f3	Clay	X	-	-	-	-	-	-	-	-	X	MA_CM
Tr-128-5_f1	Clay	X	-	-	-	-	-	-	-	-	X	MA_CM
Tr-254-2_f1	Clay	XX	-	-	-	-	-	-	-	-	X	MA_CM
Tr-1-33	-	-	MCQ	X	X	-	-	-	X	-	-	MA_MQC
Tr-128-5_f2	-	-	MCQ	XX	X	-	X	X	X	-	X	MA_MQC
Tr-161-2-3	-	-	MCQ	XX	-	-	-	-	-	-	X	MA_MQC
Tr-161-2b-2_f2	-	-	MCQ	XX	X	-	-	-	-	-	X	MA_MQC
Tr-161-2b-6	-	-	MCQ	XX	X	X	-	-	-	X	X	MA_MQC
Tr-222-12_f2	-	-	MCQ	XX	-	-	-	-	-	-	X	MA_MQC
Tr-223-3-2	-	-	MCQ	XX	-	X	-	-	X	-	X	MA_MQC
Tr-254-2_f2	-	-	MCQ	XX	X	-	-	-	-	-	X	MA_MQC
Tr-1-18	Silic.	X	-	-	-	-	-	-	X	-	-	OO
Tr-129-2-4	Silic.	X	-	-	-	-	-	-	-	-	X	OO
Tr-161-2b-2_f3	-	-	MCQ	X	-	X	-	-	-	-	X	OO
Tr-222-12_f1	-	-	MCQ	X	-	-	-	-	-	X	X	OO

Fig. 5. Matrix and cement types and quantities, mineral identification and mineral variety (bearing in mind its petrogenetic type). For cement or matrix quantification we used X for minor or trace presence in the thin section sample; XX for major presence; and XXX for very abundant presence.

Abb. 5. Matrix- und Zementtypen und -mengen, Mineralidentifizierung und Mineralienvielfalt (unter Berücksichtigung des petrogenetischen Typs). Für die Zement- oder Matrixquantifizierung wird X für geringe oder einfache Anwesenheit in der Dünnschliffprobe, XX für starke und XXX für sehr starke Anwesenheit verwendet.



**Fig. 6.** Quartz grain measurements of thin section samples. A) Histogram of the size of the particles using their second diameter and classified by the Udden-Wentworth scale (Wentworth, 1922). B) Biplot representing the morphology of quartz grains using circularity and roundness indexes. C) Circular orientation charts of samples Tr-222-12\_f3, Tr-222-12\_f2 and Tr-1-18. Grey is used for MA\_MQC, brown is used for MA\_CM and yellow for OO.

**Abb. 6.** Quarzkornmessungen an Dünnschliffproben. A) Histogramm der Größe der Partikel anhand ihres zweiten Durchmessers und klassifiziert nach der Udden-Wentworth-Skala (Wentworth, 1922). B) Biplot, der die Morphologie der Quarzkörner unter Verwendung von Zirkularitäts- und Rundheitsindizes darstellt. C) Zirkuläre Orientierungsdiagramme der Proben Tr-222-12\_f3, Tr-222-12\_f2 und Tr-1-18. Grau wird für MA\_MQC, Braun für MA\_CM und Gelb für OO verwendet.

Sample	SiO <sub>2</sub>	Al <sub>2</sub> O <sub>3</sub>	Fe <sub>2</sub> O <sub>3</sub>	MnO	MgO	CaO	Na <sub>2</sub> O	K <sub>2</sub> O	TiO <sub>2</sub>	P <sub>2</sub> O <sub>5</sub>	Method
Tr-1-18	99.37	0.192	0.128	0.001	0.035	0.033	0.018	0.044	0.048	0.027	cut
Tr-128-5	98.48	0.260	0.270	0.001	0.017	0.298	0.018	0.017	0.099	0.019	cut
Tr-129-2-4	99.54	0.128	0.080	0.001	0.017	0.013	0.042	0.017	0.115	0.009	cut
Tr-1-33	99.11	0.074	0.115	0.001	0.017	0.159	0.018	0.017	0.110	0.004	cut
Tr-161-2-3	99.63	0.085	0.187	0.001	0.017	0.013	0.018	0.017	0.057	0.004	cut
Tr-161-2b-2	99.37	0.116	0.181	0.001	0.084	0.013	0.018	0.017	0.104	0.014	cut
Tr-161-2b-6	99.63	0.123	0.131	0.001	0.017	0.013	0.018	0.017	0.054	0.012	cut
Tr-222-12	99.40	0.154	0.271	0.001	0.017	0.035	0.018	0.017	0.099	0.024	cut
Tr-223-3-2	99.57	0.114	0.091	0.001	0.017	0.013	0.018	0.017	0.127	0.061	cut
Tr-254-2	99.66	0.061	0.166	0.001	0.017	0.043	0.018	0.017	0.053	0.004	cut
Tr-1-18	96.91	0.005	0.118	0.004	0.039	0.013	0.012	0.006	0.072	0.004	bead
Tr-161-2-3	96.16	0.005	0.200	0.001	0.002	0.013	0.012	0.006	0.101	0.004	bead
Tr-222-12_f3	96.64	0.943	0.441	0.014	0.002	0.013	0.012	0.073	0.146	0.008	bead
Tr-222-12_f2	96.75	0.005	0.268	0.002	0.002	0.013	0.012	0.006	0.095	0.004	bead
Tr-222-12_f1	99.15	0.009	0.183	0.001	0.002	0.013	0.012	0.006	0.101	0.004	bead
Tr-128-5_f1	98.72	0.165	0.227	0.001	0.002	0.013	0.023	0.012	0.111	0.004	bead
Tr-128-5_f2	99.80	0.005	0.079	0.001	0.002	0.013	0.012	0.006	0.090	0.004	bead

**Fig. 7.** Major oxide concentrations (in wt %) in selected samples from Troisdorf-Ravensberg archaeological site.

**Abb. 7.** Wesentliche Oxidkonzentrationen (in Gew.-%) in ausgewählten Proben der archäologischen Fundstelle Troisdorf-Ravensberg.

very small presence of non-quartz minerals. A clearer chemical difference would only have been found, chiefly in  $Al_2O_3$  content, if samples with higher proportions of clay matrix had been selected by Palaeolithic humans.

#### **Petrogenetic types and mineralogical varieties**

Once groups, types and varieties had been established through petrographic analysis of thin sections, they were described in detail grouped by types and varieties. This information helps to understand the most-relevant features observed by non-destructive criteria.

#### ***Cemented quartz-arenite with microcrystalline quartz (MA\_MQC)***

The most abundant rock type is the matrix or cemented quartz-arenite with microcrystalline quartz (MA\_MQC). Samples Tr-1-33, Tr-128-5\_f2, Tr-161-2-3, Tr-161-2b-2\_f2, Tr-161-2b-6, Tr-222-12\_f2, Tr-223-3-2, and Tr-254-2\_f2 belong to this type. The texture of all these sandstones is clastic with matrix or cement and packing varies from isolated to tangential. The most frequent features of the quartz grains are clastic quartz grains, occasionally surrounded by syntaxial overgrowths. In some areas of the samples it is possible to recognise concavo-convex quartz grain limits (Fig. 8: B). According to grain size characterization, the most represented grain size categories are very fine and fine sand, generally with a prevalence of the very fine sand category. There is also a significant presence of smaller quartz grain sizes and some other bigger than fine sand quartz grains. The biggest quartz grain is 0.33 mm, identified in sample Tr-161-2b-6. Regarding the morphology of the particles, there is a prevalence of regular shape with high circularity indexes (Circ. >0.57) and general tendency to non-elongated shapes (Round  $\approx$ 0.62). No preferential orientation was detected in this type. The cement is chiefly composed of microcrystalline quartz, although the cryptocrystalline type is also represented, as fibrous chalcedony fillings (Fig. 8: C). The presence of microcrystalline quartz is generally between 5% and 20% of the samples and it creates a new coating on quartz grains after the first syntaxial overgrowths. In the cases where packing is less compact, the quantity of cement is higher. Among the non-quartz minerals, iron oxides are frequent, followed by zircon and clays. Iron oxides appear as small crystals inside microcrystalline quartz too. Mica, pyrite, chlorite, and rutile, are present in some samples.

Stereomicroscopic characterisation reveals that it is easy to recognise the quartz grains, which display rounded and sometimes plain quartz limits. The grains generate punctual or tangent packing and the texture is related with a fine and grainy texture due to the presence of microcrystalline quartz cement (Fig. 8: A). The latter is easy to recognise as a bright and vitreous lustre which covers and encloses the quartz grains.

Iron oxides appear in some zones of the samples, generally together with small quartz grains or inside fractures.

#### ***Clayey matrix quartz-arenite (MA\_CM)***

Samples Tr-161-2b-2\_f1, Tr-222-12\_f3, Tr-128-5\_f1 and Tr-254-2\_f1 clearly belong to this type and variety. Thin sections show that all textures are clastic with matrix or/and cement and their packing is tangential. The characterisation of grains reveals the presence of clastic quartz with syntaxial overgrowths in most grains, while concave-convex quartz grain boundaries are limited to small complete packing areas. It is possible to observe undulatory extinction in some areas of sample Tr-222-12\_f3 (Fig. 8: E). Quartz grain sizes are similar in the four samples with heterogeneous distribution. However, most of the grains are between the very fine and fine categories. The former is more frequent in sample Tr-222-12\_f3, while the latter is more represented in the other samples. The presence of smaller grains is frequent. There are also small quantities of bigger grains of up to 0.57 mm (in sample Tr-222-12). The morphology of quartz grains is generally regular. The roundness index of the particles indicates that most of the grains are not elongated. The samples Tr-222-12\_f3 and Tr-254-2\_f1 show preferential orientation at  $\alpha = 0.05$ . Regarding the mineral characterisation of the samples, the type of matrix is clayey. The latter creates a coating on quartz grains (Fig. 8: F). In the cases where cement is present, it is formed by microcrystalline quartz, generally as fibrous chalcedony and growing above the first coating of clays in between clastic quartz grains (in negligible proportions). Iron oxides are present among non-quartz minerals, probably related with the presence of clayey matrix.

Regarding the characterisation of this type and variety under binocular microscopy, it is easy to recognise floating or punctual packing surfaces and saccharoid texture (Fig. 8: D). The clayey matrix appears as small specks on the surfaces of the samples and between quartz grains. The latter are easily recognisable and their borders are well defined. Generally, they are rounded, although it is also sometimes possible to find straight quartz grain limits and angular surfaces. The presence of iron oxides on surfaces is recurrent.

#### ***Syntaxially overgrown orthoquartzite (OO type)***

The last type analysed is the OO petrogenetic type and it is described from samples Tr-1-18, Tr-129-2-4, Tr-161-2b-2\_f3, and Tr-222-12\_f1. They display clastic grained texture and complete packing although small porosity could be also observed (Fig. 8: H). The characterisation of grains reveals the coexistence of clastic grains and undulatory extinction (in different areas of the thin section). Most of the grains exhibit syntaxial overgrowths that generate concave-convex quartz grain limits (Fig. 8: I). Syntaxial overgrowths are

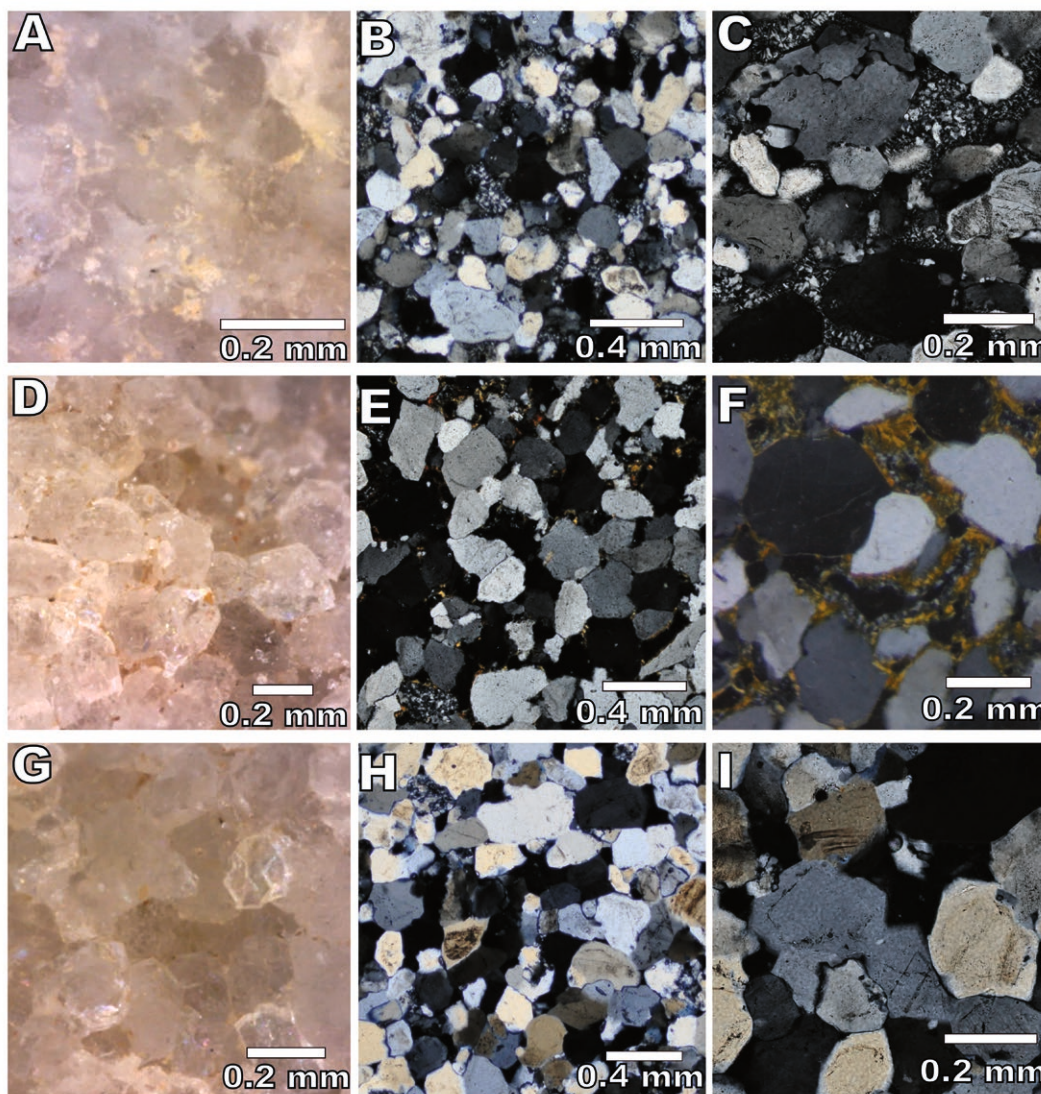


**Fig. 8.** Microphotograph of fracture surfaces at 250x magnification (A, D, and G) of quartzites from Troisdorf-Ravensberg and photomicrographs of thin sections at different magnifications. From top to bottom, MA\_MQC, MA\_CM and OO rock types. A) surface photomicrograph at 250x magnification of Tr-128-5\_f2. Grains are observable surrounded by a coating of microcrystalline siliceous cement. B) thin section photomicrograph at 50x magnification of sample Tr-128-5\_f2: Mosaic of clastic grains with some overgrowth surrounded by microcrystalline quartz cement. C) thin section photomicrograph at 200x of sample Tr-128-5\_f2. Detailed of microcrystalline and cryptocrystalline quartz. Fibrous chalcedonic variety visible at the top of the image. D) surface photomicrograph at 250x magnification of Tr-128-5\_f1. Grains are easy to recognise, also clayey matrix between them and secondary quartz frameworks. E) thin section photomicrograph at 50x magnification of sample Tr-161-2b\_2\_f1: mosaic of clastic grains with some overgrowth surrounded by clayey matrix and rock fragments. Packing is tangential. F) thin section photomicrograph at 200x of sample Tr-254-2\_f1. Matrix coating around quartz grains is covered in some empty spaces by thin layers of microcrystalline quartz. G) surface photomicrograph at 250x magnification of Tr-129-2-4. Grains are easy to recognise, also appearance of regrowth of syntaxial quartz cement. H) thin section photomicrograph at 50x magnification of sample Tr-1-18: complete mosaic of clastic grains with overgrowth and concave-convex quartz outlines. I) thin section photomicrograph at 200x of sample Tr-1-18. There is no matrix and quartz grains exhibit syntaxial overgrowth.

**Abb. 8.** Mikroaufnahmen von Bruchflächen bei 250-facher Vergrößerung (A, D und G) von Quarziten aus Troisdorf-Ravensberg und Mikroaufnahmen von Dünnschliffen bei verschiedenen Vergrößerungen. Von oben nach unten: MA\_MQC, MA\_CM und OO-Gesteinstypen. A) Oberflächenmikroskopische Aufnahme bei 250-facher Vergrößerung von Tr-128-5\_f2. Man sieht Körner, die von einer Schicht aus mikrokristallinem Kieselzement umgeben sind. B) Dünnschliff-Fotografie bei 50-facher Vergrößerung der Probe Tr-128-5\_f2: Mosaik aus klastischen Körnern mit etwas Überwucherung, umschlossen von mikrokristallinem Quarzement. C) Dünnschliff-Mikroskopaufnahme bei 200-facher Vergrößerung der Probe Tr-128-5\_f2. Detailaufnahme von mikrokristallinem und kryptokristallinem Quarz. Faserige Chalcedon-Varietät oben im Bild sichtbar. D) Oberflächenmikroskopische Aufnahme bei 250-facher Vergrößerung von Tr-128-5\_f1. Die Körner sind leicht zu erkennen, auch die tonige Matrix zwischen ihnen und den sekundären Quarzgerüsten. E) Dünnschliff-Mikroskopaufnahme bei 50-facher Vergrößerung der Probe Tr-161-2b\_2\_f1: Mosaik aus klastischen Körnern mit etwas Überwucherung, eingefasst von tonhaltiger Matrix und Gesteinsfragmenten. Die Umhüllung ist tangential. F) Dünnschliff-Mikroskopaufnahme bei 200-facher Vergrößerung der Probe Tr-254-2\_f1. Die Matrixbeschichtung um die Quarzkörner ist in einigen leeren Räumen von dünnen Schichten mikrokristallinen Quarzes bedeckt. G) Oberflächenmikroskopische Aufnahme bei 250-facher Vergrößerung von Tr-129-2-4. Die Körner sind leicht zu erkennen, auch das Nachwachsen von syntaxialem Quarz-Zement ist zu erkennen. H) Dünnschliff-Fotografie bei 50-facher Vergrößerung der Probe Tr-1-18: Vollständiges Mosaik klastischer Körner mit Überwucherung und konkav-konvexen Quarzumrissen. I) Dünnschliff-Fotografie bei 200-facher Vergrößerung der Probe Tr-1-18. Es gibt keine Matrix, und die Quarzkörner weisen eine synthetische Überwucherung auf.

thicker than in the previous two types, and it is possible to detect two different growth lines surrounding the detrital grains. Most of the grains, according to their sizes, are classified within the fine sand and very fine sand categories. The exception is sample Tr-222-12\_f1, where coarse silt is the most frequent category. The presence of smaller grains is clear and big quartz grains are less frequent than in previous types (the biggest quartz grain is 0.3 mm). The morphology of the grains is regular, displaying non-elongated shapes. No preferential orientation was detected in this type. Tr-1-18 and Tr-129-2-4 have a small portion of silica matrix grains and residual microcrystalline cement is observable in samples Tr-161-2b-2\_f3 and Tr-222-12\_f1 in negligible proportions. Iron oxides, rutile, clays and pyrite are observable in some of them.

The characterisation of surface texture as compact and grainy using the non-destructive method is clear, like the complete packing (Fig. 8: G). Rounded quartz grain limits are obvious, with some appearance of regrowth. Iron oxides are present in almost every sample, as well as some non-identified black and heavy minerals.

#### **Connecting the features: relationship in between different facies**

To understand in greater detail the processes which create the sampled rock types, the relationship between the different facies will be analysed using those samples where two or more microfacies are recognized (samples Tr-161-2b-2, Tr-222-12). In addition, specific features of sample Tr-223-3-2 will be described.

Using only non-destructive characterisation of the samples Tr-161-2b-2 and Tr-222-12 (Fig. 1: 8 & 9), we could distinguish three clear facies in the following order: 1) MA\_CM, 2) MA\_MQC, and 3) OO. These facies are easily recognisable based on lustre, texture, packing, and other features. The first facies (MA\_CM, Fig. 9: A) is situated on top of the second facies, (MA\_MQC, Fig. 9: B & C). Both facies are separated by an abrupt thin layer of iron oxides (Fig. 9:  $\alpha$ ), slightly diffused into the MA\_MQC type (Fig. 9: D). The change between both facies is clear and abrupt, easily observable by the change of lustre, from earthy to vitreous, and of the texture, from clear saccharoid texture to a fine and grainy or even fine one. Finally, the last facies, the OO type, is situated under the MA\_MQC variety (Fig. 9: E & F). The relationship between the latter two facies is not as obvious as the former one due to the progressive disappearance of microcrystalline quartz as a consequence of the increase in grain compactness because of the quartz overgrowths (Fig. 9:  $\beta$ ). In this case, the transition from a vitreous to earthy lustre is not so clear. This is also observable when progressive changes from a fine texture to a compact and grainy one take place. These relationships are similar in other samples not selected for the petrographic characterisation.

The petrographic characterisation of the samples emphasised the existing relationship between the three facies, as observed on the cut surface of sample Tr-222-12 (Fig. 10). The upper one is formed by the MA\_CM facies, the central one is the MA\_MQC, and the lower facies is the OO type. Regarding the first, the thin section shows the main presence of clayey matrix with many oxides that fill the space between quartz grains in the MA\_CM part (Fig. 10: B). The microcrystalline quartz, even the chalcedonic phases, does not cover quartz grains, but the clayey coating around the quartz grains. In the outer areas it is possible to observe black and undefined minerals as a consequence of the weathering process. The inner areas are relatively homogeneous and we do not observe gradation or different zones because of the presence of cement, matrix, textural relationship or the morphology and size of grain. The abrupt change between two varieties of MA types is emphasised in the fresh cut as figure 10:  $\alpha$  shows. The contact consists of a lighter thin area that clearly separates both layers. In thin section, microcrystalline quartz disappears in the small transition zone from MA\_MQC type to MA\_CM (Fig. 10: A). Focusing on the MA\_MQC facies, the colour is generally heterogeneous, ranging from grey and lighter areas to orange zones in the freshly cut surface. Petrographic characterisation shows the major presence of microcrystalline quartz filling the pores or spaces between quartz grains (Fig. 10: C & D). These spaces have no matrix, but a small proportion of oxides in specific zones. The OO facies is not clearly distinguished from the layer above it. There is no separating stratum, nor neat change between both facies. The change between MA\_MQC and OO types is gradual and determined by progressive change in packing, from tangential to complete categories as a consequence of the syntaxial quartz overgrowths, more numerous and bigger in the OO than in the MA\_MQC (Fig. 10: E & F). This gradation progressively blocks the entrance of microcrystalline quartz from the MA\_MQC facies to the OO one, generating transitional zones until the complete absence of microcrystalline quartz cement (Fig. 10:  $\beta$ ).

The last sample analysed to understand the relationship between the three types and varieties is Tr-223-3-2. Other examples of these pores suggest this feature could be related to rootlet marks. The sample here analysed corresponds to the MA\_MQC variety and it is the only sample with clear presence of pores or chimneys filled with microcrystalline quartz cement (Fig. 11). This sample evidences groundwater circulation and the precipitation of the silica, and other dissolved minerals, using the space created by different structures, such as rootlets. From those places, microcrystalline quartz fills the space between quartz grains, adapting to their shapes. It is important to note that no chalcedonic quartz is observed in this sample.

## Discussion

### Understanding rock formation

As stated above, one of the objectives of this research is to describe and characterise the different facies we observed in the Tertiary quartzite from Troisdorf-Ravensberg using a multi-focus approach based on geoarchaeological methods. All three described types show features clearly related with sedimentary

processes and not with metamorphism. The absence of metamorphic textures in all selected samples, like foam textures, recrystallised quartz grains, Böhm lamellae, fractures inside grains or even microstylolitic borders, reinforces the sedimentary character of these rocks. Nevertheless, these metamorphic features have been previously described in quartzites knapped by Palaeolithic people in other regions, such as in Iberia (Pedergrana et al. 2017; Prieto et al. 2019) or in the

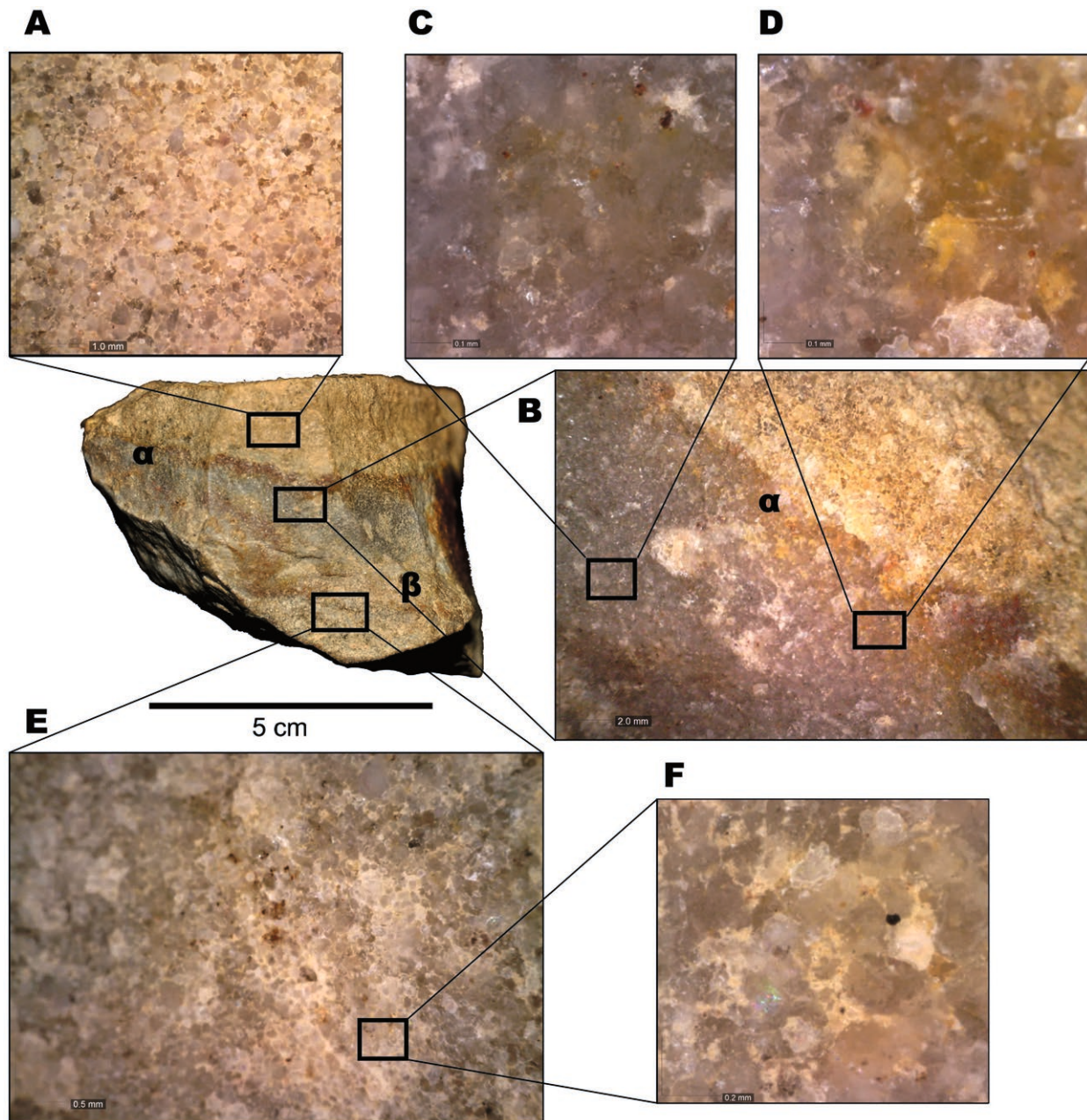


**Fig. 9.** Picture of sample Tr-161-2b-2 and photomicrographs of its surfaces at different magnifications. The source area of each photomicrograph is indicated in the general picture. A: Detail of MA\_CM at 50x magnification. B: MA\_MQC and transition with the MA\_CM zones at 20x magnification. C: MA\_MQC area without oxides at 250x magnification. D: MA\_MQC area with oxides at 250x magnification. E and F: OO facies at 20x and 250x magnification.  $\alpha$ : Limit between MA\_CM and MA\_MQC facies.  $\beta$ : Limit between MA\_MQC and OO facies.

**Abb. 9.** Abbildung der Probe Tr-161-2b-2 und Mikrofotoaufnahmen ihrer Oberflächen bei verschiedenen Vergrößerungen. Der Quellbereich jeder Mikrofotografie ist im allgemeinen Überblicksbild angegeben. A: Detail von MA\_CM bei 50-facher Vergrößerung. B: MA\_MQC und Übergang mit den MA\_CM-Zonen bei 20-facher Vergrößerung. C: MA\_MQC-Bereich ohne Oxide bei 250-facher Vergrößerung. D: MA\_MQC-Bereich mit Oxiden bei 250-facher Vergrößerung. E und F: OO-Fazies bei 20-facher und 250-facher Vergrößerung.  $\alpha$ : Grenze zwischen MA\_CM- und MA\_MQC-Fazies.  $\beta$ : Grenze zwischen MA\_MQC- und OO-Fazies.

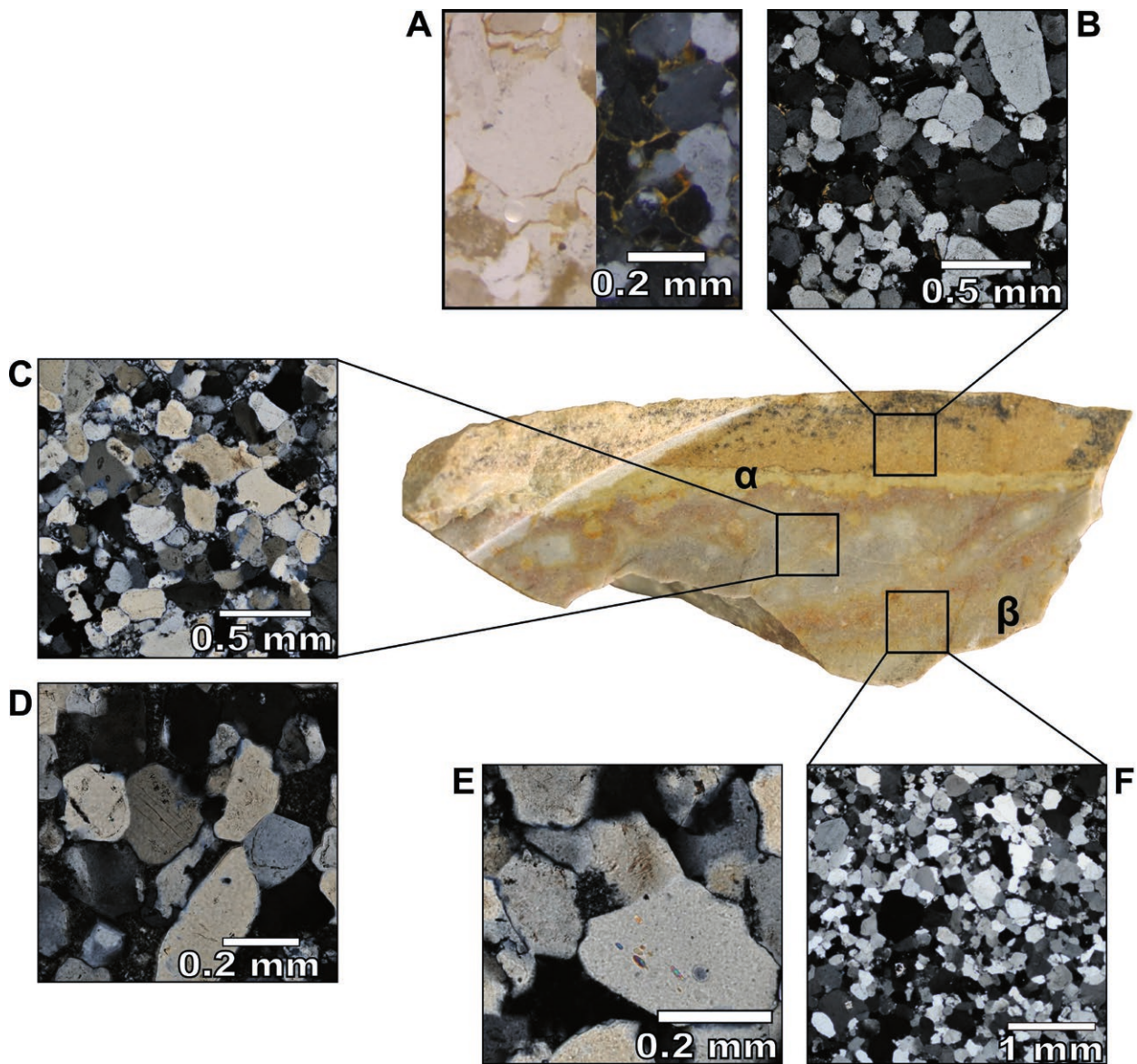


**Fig. 10.** Picture of sample Tr-222-12 after being cut for thin section. Thin sections at diverse magnifications are also shown. The source area of each photomicrograph is indicated in the general picture. A: Detail of the thin section at the limit between MA\_CM and MA\_MQC areas. Note that clay is the main component of the matrix. A small part of microcrystalline quartz can be observed. B: Thin section of the MA\_CM area. C: Thin section photograph of the MA\_MQC area. D: Detail of the thin section of the microcrystalline quartz cement and the relationship with grain framework. E: Thin section photograph of the OO area. F: Detail of the thin section of the OO area, exhibiting concavo-convex quartz grain limits and presence of syntaxial regrowth.  $\alpha$ : Limit between MA\_CM and MA\_MQC facies.  $\beta$ : Limit between MA\_MQC and OO facies.

**Abb. 10.** Abbildung der Probe Tr-222-12 nach dem Zuschnitt für den Dünnschliff. Ebenfalls dargestellt sind Dünnschliffe in verschiedenen Vergrößerungen. Der Quellbereich jeder Mikrofotografie ist im allgemeinen Überblicksbild angegeben. A: Detail des Dünnschliffs an der Grenze zwischen den Bereichen MA\_CM und MA\_MQC. Man beachte, dass Ton die Hauptkomponente der Matrix ist. Ein kleiner Teil des mikrokristallinen Quarzes kann beobachtet werden. B: Dünnschliff des MA\_CM-Bereichs. C: Dünnschliffbild des MA\_MQC-Bereichs. D: Detail des Dünnschliffs des mikrokristallinen Quarzements und die Beziehung zum Korngerüst. E: Dünnschliffbild des OO-Bereichs. F: Detail des Dünnschliffs des OO-Bereichs, der konkav-konvexe Quarzkorngrenzen und das Vorhandensein von syntaxialer Nachwachsung zeigt.  $\alpha$ : Grenze zwischen MA\_CM- und MA\_MQC-Fazies.  $\beta$ : Grenze zwischen MA\_MQC- und OO-Fazies.

Rift Valley in Africa (Soto et al. 2020). The presence of clastic grained texture (with and without matrix or cement), detrital quartz grains, syntaxially quartz overgrowths or concave-convex quartz grain limits described in this research clearly represent sedimentary processes. Some of these sedimentary features were also characterised in quartzites related with other archaeological contexts and were described

for sites from Belgium (Blomme et al. 2012; Cnudde et al. 2013; Veldeman et al. 2012), the Iberian Peninsula (Prieto et al. 2019; Roy et al. 2017) or North America (Dalpra & Pitblado 2016). Therefore, the characterisation of these Tertiary quartzites as a material derived from sedimentary forces underscores the variability of rocks described under the term of quartzite by archaeologist.

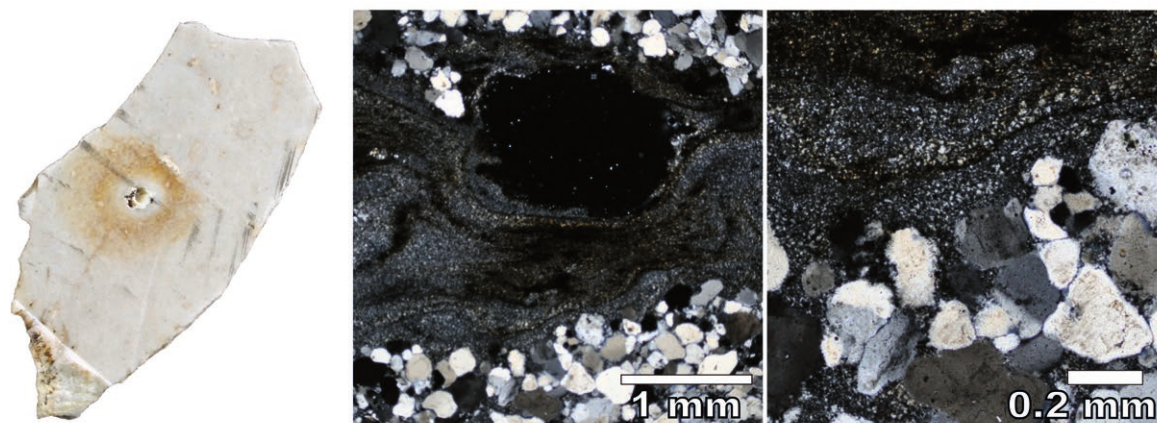


**Fig. 11.** Photograph at different magnification of sample Tr-223-3-2. The first one shows the sample after being cut for thin section preparation. The porosity where microcrystalline quartz is massively trapped as well as the concentric oxides around it is easily observable. The following two thin sections display microcrystalline quartz grains in the big pore and the filling process of the general MA type porosity. Fe oxides colouring areas of the microcrystalline quartz grains are also identified.

**Abb. 11.** Abbildungen bei unterschiedlicher Vergrößerung der Probe Tr-223-3-2. Das erste Bild zeigt die Probe nach dem Zuschnitt für die Dünnschliffpräparation. Die Porosität, in der mikrokristalliner Quarz massiv eingeschlossen ist, sowie die konzentrischen Oxide um ihn herum sind leicht zu erkennen. Die folgenden beiden Dünnschliffe zeigen mikrokristalline Quarzkörner in der großen Pore und den Füllvorgang der allgemeinen MA-Typ-Porosität. Es werden auch Bereiche der Färbung der mikrokristallinen Quarzkörner durch Eisenoxide identifiziert.

The formation processes of these quartzites are thought to be related with the formation of silcretes (Nash & Ulliyott 2007; Thiry & Milnes 2017; Thiry et al. 1988; Thiry et al. 2013; Ulliyott & Nash 2016; Webb & Domanski 2008) rather than with other processes, including *in situ* dissolution of sponges or volcanic rock fragments (Block Vagle et al. 1994; Lima & De Ros 2002; Vagle et al. 1994; Weibel et al. 2010). Following the definition of Eggleton (2001), highlighted by Thiry and Milnes (2017: 1), silcrete could be defined as a "strongly silicified, indurated regolith, generally of low permeability, commonly having a conchoidal fracture with a vitreous lustre. Represents the complete or near-complete silicification of regolith by the transformation of precursor silica or silicates and/or the infilling of available voids, including fractures. On a macroscopic scale, some silcretes are dense and massive, but others may be nodular, columnar, blocky, or cellular with boxwork structure. On a microscopic scale, the fabric, mineralogy and composition of silcretes may reflect those of the parent material, but also indicate the changes experienced by, as well as the general environments of, silicification".

This explanation perfectly defines the material analysed in the archaeological site of Troisdorf-Ravensberg. The facies described, the behaviour of the transitional zones and some of the features characterised are part of the complex silcrete formation process. Despite the problems highlighted by some authors (Thiry & Milnes 2017; Ulliyott & Nash 2016; Ulliyott et al. 2015) and the absence of fieldwork which could contribute to a better description of this silcrete, we consider this type could be related with groundwater circulation silcrete rather than a pedogenic one (Thiry et al. 1988). These sedimentary processes based on silicification related to groundwater

circulation were also highlighted by previous regional studies of the area in the field (e.g. Floss 1990; Skupin & Wold 2011; Udluft & Pfeffer 1977; Winterscheid & Kvaček 2016). The source area of the silica could be the almost pure unconsolidated quartz sand of the *Kölner Schichten* (Köln Formation). Following the Thiry and Milnes (2017) classification, these types of "Tertiary quartzites" are associated with a complex sandstone cementation type, inserted in the proper term of silcretes. There are many examples in different parts of the world in which this raw material was used in knapping activities by hunter-gatherer societies, as recently published in the guest editorial of a Special Issue about silcretes (Wragg Sykes & Will 2017).

#### Physical properties of "Tertiary quartzites"

One of the main objectives of this research is to identify the possible traits of the procurement mechanisms applied at the site. Regarding human exploitation of "archaeological quartzites" in the site of Troisdorf-Ravensberg, we intend to identify and classify the physical (knapping) properties of the studied material (derived from petrological characterisation).

Regarding the physical properties, the three facies have similar quartz grain size features, with a main distribution between the very fine sand and the fine sand categories. Nevertheless, the presence of smaller and clearly bigger quartz grains creates non-homogeneous surfaces, promoting discontinuities in strength propagation on solid materials and lower compressive strength. Therefore, this grain size heterogeneity and the big size of particles potentially hamper knapping activities, as proposed by several authors on similar silica-based raw materials (e.g. Andrefsky 2005: 52-53 & 58; Mardon et al. 1990; Pedergnana et al. 2017;

Prieto 2018: 530-531; Webb & Domanski 2008). It is important to mention that quartz grain size in quartzites from other archaeological contexts is generally more homogeneous and slightly smaller, which promotes a higher compressive strength on them (Prieto et al. 2019, 2020).

The compactness degree of the main grain framework in the two varieties of the MA type also creates non-homogeneous surfaces. However, the major presence of microcrystalline cement in the MA\_MQC variety creates homogeneous and compact rocks that prevent the creation of pores and grain irregularities, making it a more isotropic material with higher compressive strength and less tough material, which potentially eases knapping activities (Domanski et al. 1994; Webb & Domanski 2008). According to Thiry & Milnes (2017), microcrystalline cement gives rise to strong cementation, creating bonding between the detrital quartz grains and the silica precipitates, and making complex intercrystallite connections in the pore space. Rock fractures after knapping tend to be clean, because they cut across the detrital quartz, creating conchoidal and lustrous surfaces. The differences are clear when observing the surfaces of these two varieties under the binocular (Figs. 8 & 9). In addition, the presence of microcrystalline quartz cement, but especially the breakable quartz grains, also create sharp and hard edges of flaking products promoting longer life edges (Abrunhosa, A. et al. 2019; Pederagnana et al. 2017; Thiry & Milnes 2017; Webb & Domanski 2008). As proposed by Schmidt et al. (2013), fire treatment could improve the knapping properties of some varieties of this raw material (Schmidt & Mackay 2016). Nevertheless, we do not observe traces of heating at the site. Further analysis could test this hypothesis. The knapping property of the MA\_CM facies is clearly different, despite the small relicts of microcrystalline quartz in it. This is because the matrix that coats the quartz grains creates brittle connections between quartz grains and the relicts of microcrystalline quartz (Andrefsky 2005: 52-53; Prieto 2018; Prieto et al. 2020; Webb & Domanski 2008). Therefore, and in addition to the problem of knapping stated below, the composition of the matrix hampers knapping and use processes (Pederagnana et al. 2017).

Finally, although the degree of packing in the OO type prevents porosity, which usually leads to reduced knapping properties caused by the empty space between grains, it does not prevent the irregularities generated by the differences in the size of the quartz grains (Thiry & Milnes 2017). The syntaxial cement overgrowths expanded from quartz grains and they are not welded to the main grain framework. Therefore, despite providing cohesion and hardness, they do not bond. As a result, when broken, the fractures tend to follow the overgrowth quartz cement that makes contact between grains, and they do not cross grains and overgrowths, as in MA\_MQC

(Thiry & Milnes 2017; Webb & Domanski 2008), in highly-deformed orthoquartzites or in recrystallised quartzites (Andrefsky 2005: 57-58; Prieto, 2018). A more isotropic material is obtained only in those cases where microcrystalline cement fills the small spaces between quartz grains in the OO types. This becomes an optimal knapping product.

First observation of technical procedures in this assemblage could be related with the extraction and exploitation of MA\_MQC as the primary product, the secondary exploitation of the OO type (especially with a small quantity of microcrystalline quartz) as a by-product, and the discard of MA\_CM as a waste product. The impression is that flaking surfaces are more frequent in the MA\_MQC variety and the OO type. This is observable in the stones, which still preserve the three facies, such as those observed in figure 1: 9 & 10. Another example of this selective exploitation is observable in zones where rootlets (filled by microcrystalline quartz) are present. Usually, areas around them show negative scars, probably as a consequence of the intensive exploitation of these areas, generally with a higher presence of microcrystalline quartz cement (Fig. 1: 2). These hypotheses are in line with previous research on the site that characterises it as a workshop where first stages of the reduction process have been made (Pastoors et al. 2016; Fiedler & Veil 1974). Moreover, and as already suggested, these hypotheses must be confirmed by follow-up research (Prieto 2020).

## Conclusions

This research has tried to understand the physical properties of the quartzites as an important aspect to understand the raw material procurement strategies carried out by the humans who inhabited the middle-lower Rhine Valley (Germany). We have therefore characterized the Tertiary quartzites from the site of Troisdorf-Ravensberg using a solid geoarchaeological procedure. We have applied similar procedures to those already used by our team to describe the quartzite in the Cantabrian Region (Prieto et al. 2019, 2020). We consider that the application of this method in a different region and, especially, in a different type of rock: a silcrete, reinforces its validity. It also reinforces the idea that the term "quartzite" used by archaeologists veils a more complex geological reality that ranges from sedimentary to metamorphic realms.

Petrographic and petrological characterisation points to the presence of three different facies of quartzites in the lithic assemblage. None of them display evidence of recrystallisation generated by metamorphic forces, and only one has minor evidence of deformation. This type belongs to the type of Syntaxially Overgrowth Orthoquartzite, OO. The other two facies are clastic or cemented quartzarenites (MA). One of them, the MA\_CM one, is characterised by the presence of matrix and the other by

microcrystalline quartz cement. The latter cement could also be represented in small proportions in the OO type. The presence of this microcrystalline quartz in the MA\_MQC makes this rock optimal for knapping and use. Thus, its massive exploitation could be the main reason for human activity in this site.

Future research will pursue the exciting question of whether one of the three facies of quartzites, and if so which one, was predominantly extracted in Troisdorf-Ravensberg. After the first impressions it seems that the main focus was on the exploitation of the MA\_MQC facies. The use and acquisition of the OO type would be secondary and derived from the main product, MA\_MQC facies. The knapping properties of the MA\_CM variety are not good. It will be interesting to evaluate these first impressions with results based on empirical data from the complete assemblage.

The conclusions reached here, probably enriched by additional potential behavioural patterns deduced from future research by applying the technological characterisation of the assemblage, reinforce that this location was an important place for the Middle Palaeolithic population of the Lower Rhine Valley (Fiedler & Veil 1974; Pastoors et al. 2016). This conclusion is similar to those described and analysed by other researchers at Middle Palaeolithic sites in the east-central Massif Central in France (Wragg Sykes et al. 2017), in the central part of Iberia (Baena et al. 2011), in Egypt (Van Peer et al. 2010) and in the Near and Middle East (Finkel et al. 2019; Groucutt et al. 2017). The recurrent use of these sites for raw material acquisition makes them important landmarks for Palaeolithic populations (Barkai & Gopher 2009). This hypothesis points not only to selective extraction of specific rock, but also to other aspects of the procurement strategies connected with human mobility, transportation of raw materials and planned spatial management of the environment. A better comprehension of these aspects, through the analysis of this type of silcrete in other archaeological sites and geological localities in the Lower Rhine Valley, could contribute towards a better insight into the procurement strategies followed by Middle Palaeolithic populations in this region (Prieto 2020).

**ACKNOWLEDGEMENTS:** The authors would like to thank the Department of Mineralogy and Petrology of UPV/EHU for access to the laboratories, thin-section preparation and X-Ray fluorescence analysis at the SGIker Facilities. This research was partially supported by the project HAR2017-82483-C3-1-P financed by the Spanish Ministry of Science and the Consolidated Research Group in Prehistory of the Basque Country University (IT-1223-19). A. Prieto is also part of this project and he is a member of the research group. He is also a collaborator in the project HAR2016-76760-C3-2-P funded by the Spanish Ministry of Science and FEDER funds. A. Prieto is funded by the Education Department of the Government of the Basque Country through a postdoctoral fellowship (POS\_2018\_1\_0021).

## Literature cited

- Abrunhosa, A., Pereira, T., Márquez, B., Baquedano, E., Arsuaga, J. L., & Pérez-González, A. (2019). Understanding Neanderthal technological adaptation at Navalmaillo Rock Shelter (Spain) by measuring lithic raw materials performance variability. *Archaeological and Anthropological Sciences*, 11(11), 5949-5962.
- Andrefsky, W. (2005). *Lithics. Macroscopic Approaches to Analysis* (Second Edition ed.). Cambridge University Press, Cambridge, New York, Melbourne, Madrid, Cape Town, Sao Paulo.
- Baena, J., Báñez, S., Pérez-González, A., Roca, M., Lázaro, A., Márquez, R., Rus, I., Manzano, C., Cuartero, F., Ortiz, I., Rodríguez, P., Pérez, T., González, I., Polo, J., Rubio, D., Alcaraz, M. & Escobar, A. (2011). Searchers and miners: first signs of Flint exploitation in Madrid's region. In: M. Capote, S. Consuegra, P. Díaz-del-Río, & X. Terradas (Eds.), *Proceedings of the 2nd International Conference of the UISPP Commission on Flint Mining in Pre- and Protohistoric Times (Madrid, 14-17 October 2009)*. Archaeopress Publishers of British Archaeological Reports BAR, Oxford, 203-220.
- Bamforth, D. B. (2006). The Windy Ridge quartzite quarry: hunter-gatherer mining and hunter-gatherer land use on the North American Continental Divide. *World Archaeology* 38 (3): 511-527.
- Barkai, R. & Gopher, A. (2009). Changing the face of the earth: human behaviour at Sede Ilan, an extensive lower-middle Palaeolithic quarry site in Israel. In: B. Adams & B. Blades (Eds.), *Lithic materials and Palaeolithic societies*. Blackwell, Oxford, 174-185.
- Binford, L. R. (1979). Organization and formation processes: looking at curated technologies. *Journal of Anthropological Research* 35: 255-273.
- Block Vagle, G., Hurst, A. & Dypvik, H. (1994). Origin of quartz cements in some sandstones from the Jurassic of the Inner Firth (UK). *Sedimentology* 41: 363-377.
- Blomme, A., Degryse, P., Van Peer, P. & Elsen, J. (2012). The characterization of sedimentary quartzite artefacts from Mesolithic sites, Belgium. *Geologica Belgica* 15 (3): 193-199.
- Brantingham, P. (2003). A neutral model of stone raw material procurement. *American Antiquity* 68(3): 487-509.
- Cnudde, V., Dewanckele, J., De Kock, T., Boone, M., Baele, J. M., Crombé, P. & Robinson, E. (2013). Preliminary structural and chemical study of two quartzite varieties from the same geological formation: a first step in the sourcing of quartzites utilized during the Mesolithic in northwest Europe. *Geologica Belgica* 16 (1-2): 27-34.
- Daffara, S., Berruti, G. L. F., Berruto, G., Eftekhari, N., Vaccaro, C. & Arzarello, M. (2019). Raw materials procurement strategies at the Ciota Ciara cave: New insight on land mobility in north-western Italy during Middle Palaeolithic. *Journal of Archaeological Science: Reports* 26: 101882.
- Dalpra, C. L., & Pitblado, B. L. (2016). Discriminating Quartzite Sources Petrographically in the Upper Gunnison Basin, Colorado: Implications for Paleoamerican Lithic-Procurement Studies. *PaleoAmerica* 2 (1): 1-10.
- Davis, J. C. (1986). *Statistics and data analysis in Geology* (Second edition ed.). John Wiley & Sons, New York, Chichester, Brisbane, Toronto, Singapore.
- Domanski, M., Webb, J. A. & Boland, J. (1994). Mechanical properties of stone artefact materials and the effect of heat treatment. *Archaeometry*, 36(2), 177-208.
- Doronicheva, E., & Shackley, S. (2014). Obsidian Exploitation Strategies in the Middle and Upper Palaeolithic of the Northern Caucasus: New Data from Mesmaiskaya Cave. *PaleoAnthropology* 2014: 565-585.
- Eggleton, R. A. (2001). *Regolith glossary: surficial geology, soils and landscapes*. Cooperative Research Centre for Landscape Evolution and Mineral Exploitation, Canberra.

- Fernandes, P., Raynal, J.-P. & Moncel, M.-H. (2008).** Middle Palaeolithic raw material gathering territories and human mobility in the southern Massif Central, France: first results from a petro-archaeological study on flint. *Journal of Archaeological Science* 35 (8): 2357-2370.
- Fiedler, L. & Veil, S. (1974).** Ein steinzeitlicher Werkplatz mit Quarzitarfakten vom Ravensberg bei Troisdorf, Siegkreis. *Bonner Jahrbuch* 174: 378-407.
- Finkel, M., Barkai, R., Gopher, A., Tirosh, O. & Ben-Yosef, E. (2019).** The "Flint Depot" of prehistoric northern Israel: Comprehensive geochemical analyses of flint extraction and reduction complexes and implications for provenance studies. *Geoarchaeology* 34 (6): 661-683.
- Floss, H. (1990).** *Rohmaterialversorgung im Paläolithikum des Mittelrheingebietes*. P.D., dissertation, Universität zu Köln, Habelt, Bonn.
- Gómez de Soler, B., Chacón, M. G., Bargalló, A., Romagnoli, F., Soto, M., Vallverdú, J. & Vaquero, M. (2019).** Mobilité territoriale pendant le Paléolithique moyen en contextes discoïde et Levallois: exemple du site de l'Abric Romaní (Capellades, Barcelona, Espagne), niveau M et sous-niveau Oa. In: M. Deschamps, S. Costamagno, P.-Y. Milcent, M. Pétilion, C. Renard, & N. Valdeyron (Eds.), *La conquête de la montagne: des premières occupations humaines à l'anthropisation du milieu*. Éditions du Comité des travaux historiques et scientifiques, Paris.
- Gopher, A. & Barkai, R. (2014).** Middle Paleolithic open-air industrial areas in the Galilee, Israel: The challenging study of flint extraction and reduction complexes. *Quaternary International* 331: 95-102.
- Gould, R. (1978).** The anthropology of human residues. *American Anthropologist* 80 (4): 215-235.
- Groucutt, H. S., Scerri, E. M. L., Amor, K., Shipton, C., Jennings, R. P., Parton, A., Clark-Balzan, L., Alsharekh, A. & Petraglia, M. D. (2017).** Middle Palaeolithic raw material procurement and early stage reduction at Jubbah, Saudi Arabia. *Archaeological Research in Asia* 9: 44-62.
- Howard, J. L. (2005).** The Quartzite Problem Revisited. *The Journal of Geology* 113 (6): 707-713.
- Lima, R. D. & De Ros, L. F. (2002).** The role of depositional setting and diagenesis on the reservoir quality of Devonian sandstones from the Solimões Basin, Brazilian Amazonia. *Marine and Petroleum Geology* 19 (9): 1047-1071.
- Mardia, K. V. (1975).** Statistics of Directional Data. *Journal of the Royal Statistical Society. Series B (Methodological)* 37 (3): 349-393.
- Mardon, D., Kronenberg, A. K., Handin, J., Friedman, M., & Russell, J. E. (1990).** Mechanisms of fracture propagation in experimentally extended Sioux quartzite. *Tectonophysics*, 182(3), 259-278.
- Nash, D. J. & Ulliyott, J. S. (2007).** Silcrete. In: D. J. Nash & S. J. McLaren (Eds.), *Geochemical Sediments and Landscapes*. Blackwell, Oxford, 95-143.
- Pastors, A., Claßen, E., Peresani, M. & Vaquero, M. (2016).** Die mittelpaläolithische Steinbearbeitungswerkstatt am Ravensberg bei Troisdorf im Licht neuer Forschung. *Archäologie im Rheinland* 2015: 64-66.
- Pedergrana, A., García-Antón, M. D. & Ollé, A. (2017).** Structural study of two quartzite varieties from the Utrillas facies formation (Olmos de Atapuerca, Burgos, Spain): From a petrographic characterisation to a functional analysis design. *Quaternary International* 433 (Part A): 163-178.
- Pitblado, B., Cannon, M., Neff, H., Dehler, C. & Nelson, S. (2012).** LA-ICP-MS Analysis of Quartzite from the Upper Gunnison Basin, Colorado. *Journal of Archaeological Science* 40: 2196-2216.
- Prieto, A. (2018).** *Procurement and management of quartzite in the Cantabrian Region: The Middle and Upper Palaeolithic in the Deva, Cares and Güeña Valleys*. Ph.D., dissertation, Universidad del País Vasco, Vitoria-Gasteiz.
- Prieto, A. (2020).** From Cantabrian Region to Central Europe: economic territories and acquisition and management of quartzite by Palaeolithic societies. In: D. Mischna, A. Grüner, C. Reinhardt, T. Uthmeier, & U. Versteegen (Eds.), *Vom Untergrund ins Internet*. Erlangen, 120-122.
- Prieto, A., Yusta, I. & Arrizabalaga, A. (2019).** Defining and Characterizing Archaeological Quartzite: Sedimentary and Metamorphic Processes in the Lithic Assemblages of El Habario and El Arteu (Cantabrian Mountains, Northern Spain). *Archaeometry* 61 (1): 14-30.
- Prieto, A., Yusta, I. & Arrizabalaga, A. (2020).** From petrographic analysis to stereomicroscopic characterisation: a geoarchaeological approach to identify quartzite artefacts in the Cantabrian Region. *Archaeological and Anthropological Sciences* 12 (1): 32.
- Roy, M., Mora, R., Plasencia, F. J., Martínez-Moreno, J. & Benito-Calvo, A. (2017).** Quartzite selection in fluvial deposits: The N12 level of Roca dels Bous (Middle Palaeolithic, southeastern Pyrenees). *Quaternary International* 435, 49-60.
- Schmidt, P. & Mackay, A. (2016).** Why Was Silcrete Heat-Treated in the Middle Stone Age? An Early Transformative Technology in the Context of Raw Material Use at Mertenhof Rock Shelter, South Africa. *PLoS ONE* 11 (2): e0149243.
- Schmidt, P., Porraz, G., Slodczyk, A., Bellot-gurlet, L., Archer, W. & Miller, C. E. (2013).** Heat treatment in the South African Middle Stone Age: temperature induced transformations of silcrete and their technological implications. *Journal of Archaeological Science* 40 (9): 3519-3531.
- Skolnick, H. (1965).** The quartzite problem. *Journal of Sedimentary Petrology* 35 (1): 12-21.
- Skupin, K. & Wold, M. (2011).** 5108 Köln-Porz. Geologischer Dienst Nordrhein-Westfalen, Krefeld.
- Soto, M., Favreau, J., Campeau, K., Carter, T., Abtosway, M., Bushozi, P. M., Clarke, S., Durkin, P. R., Hubbard, S. M., Inwood, J., Itambu, M., Koromo, S., Larter, F., Lee, P., Mwambwiga, A., Nair, R., Olesilau, L., Patalano, R., Tucker, L. & Mercader, J. (2020).** Fingerprinting of quartzitic outcrops at Oldupai Gorge, Tanzania. *Journal of Archaeological Science: Reports* 29: 102010.
- Thiry, M. & Milnes, A. (2017).** Silcretes: Insights into the occurrences and formation of materials sourced for stone tool making. *Journal of Archaeological Science: Reports* 15: 500-513.
- Thiry, M., Ayrault, M. B. & Grisoni, J. C. (1988).** Ground-water silicification and leaching in sands: Example of the Fontainebleau Sand (Oligocene) in the Paris Basin. *Bulletin of the Geological Society of America* 100 (8): 1283-1290.
- Thiry, M., Schmitt, J.-M., Innocent, C. & Cojan, I. (2013).** Sables et Grès de Fontainebleau: Que reste-t-il des faciès sédimentaires initiaux? In: *14ème Congrès Français de Sédimentologie, Paris 2013, Trois excursions géologiques en région parisienne, Livre d'excursions*, Paris, 37-90.
- Turq, A., Roebroeks, W., Bourguignon, L. & Faivre, J.-P. (2013).** The fragmented character of Middle Palaeolithic stone tool technology. *Journal of Human Evolution* 65 (5): 641-655.
- Turq, A., Faivre, J.-P., Gravina, B. & Bourguignon, L. (2017).** Building models of Neanderthal territories from raw material transports in the Aquitaine Basin (southwestern France). *Quaternary International* 433 (Part B): 88-101.
- Udluft, H. & Pfeffer, P. (1977).** 5109 Lohmar. Geologischer Dienst Nordrhein-Westfalen, Krefeld.
- Ulliyott, J. S. & Nash, D. J. (2016).** Distinguishing pedogenic and non-pedogenic silcretes in the landscape and geological record. *Proceedings of the Geologists' Association* 127 (3): 311-319.
- Ulliyott, J. S., Nash, D. J. & Huggett, J. M. (2015).** Cap structures as diagnostic indicators of silcrete origin. *Sedimentary Geology* 325: 119-131.
- Vagle, G. B., Hurst, A. & Dypvik, H. (1994).** Origin of quartz cements in some sandstone from the Jurassic of the Inner Moray Firth (UK). *Sedimentology* 41: 363-377.

- Vaquero, M. & Romagnoli, F. (2017). Searching for Lazy People: the significance of expedient behaviour in the interpretation of Palaeolithic assemblages. *Journal of Archaeological Method and Theory* 25: 334-367.
- Van Peer, P., Vermeersch, P. M. & Paulissen, E. (2010). *Chert quarrying, lithic technology and a modern human burial at the Palaeolithic site of Taramsa 1, Upper Egypt*. Leuven University Press, Leuven.
- Veldeman, I., Baele, J. M., Goemaere, E., Deceukelaire, M., Dusar, M. & De Doncker, H. (2012). Characterizing the hypersiliceous rocks of Belgium used in (pre-)History: a case study on sourcing sedimentary quartzites. *Journal of Geophysics and Engineering* 9: 118-128.
- Webb, J. A. & Domanski, M. (2008). The relationship between lithology, flaking properties and artefact manufacture for Australian silcretes. *Archaeometry* 50 (4): 555-575.
- Weibel, R., Friis, H., Kazerouni, A. M., Svendsen, J. B., Stokkendal, J. & Poulsen, M. L. K. (2010). Development of early diagenetic silica and quartz morphologies — Examples from the Siri Canyon, Danish North Sea. *Sedimentary Geology* 228 (3): 151-170.
- Wentworth, C. K. (1922). A scale of grade and class terms for clastic sediments. *Journal of Geology* 30: 377-392.
- Winterscheid, H. & Kvaček, Z. (2016). Late Oligocene macrofloras from fluvial siliciclastic facies of the Köln Formation at the south-eastern border of the Lower Rhine Embayment (North Rhine-Westphalia, Germany). *Acta paleobotánica* 56 (1): 4-64.
- Wragg Sykes, R. M., Delvigne, V., Fernandes, P., Piboule, M., Lafarge, A., Defive, E., Santagata, C. & Raynal, J. P. (2017). "Undatable, unattractive, redundant"? The Rapavi silcrete source, Saint-Pierre-Eynac (Haute-Loire, France): Challenges studying a prehistoric quarry-workshop in the Massif Central mountains. *Journal of Archaeological Science: Reports*, 15: 587-610.
- Wragg Sykes, R. M. & Will, M. (2017). Guest editorial – Silcrete as a lithic raw material in global context: Geology, sourcing and prehistoric techno-economics. *Journal of Archaeological Science: Reports* 15: 492-499.
- Zitzmann, A., Linder, B., Steuerwald, K. & Wrede, V. (2002). *CC 5502 Köln*. Bundesanstalt für Geowissenschaften und Rohstoffe, Hannover.

## Inhalt - Contents

- Exploitation of the natural environment by Neanderthals from Chagyrskaya Cave (Altai)**  
*Nutzung der natürlichen Umwelt durch Neandertaler der Chagyrskaya-Höhle (Altai)*  
 Ksenia A. KOLOBOVA, Victor P. CHABAI, Alena V. SHALAGINA, Maciej T. KRAJCARZ, Magdalena KRAJCARZ, William RENDU, Sergei V. VASILIEV, Sergei V. MARKIN & Andrei I. KRIVOSHAPKIN.....7-31
- Petrological characterisation of the "Tertiary quartzites" from the site of Troisdorf-Ravensberg (North Rhine-Westphalia, Germany): first insights in Middle Palaeolithic outcrop exploitation**  
*Petrologische Charakterisierung der „tertiären Quarzite“ von Troisdorf-Ravensberg (Nordrhein-Westfalen, Deutschland): Erste Einblicke in die Nutzung des mittelpaläolithischen Aufschlusses*  
 Alejandro PRIETO, Iñaki YUSTA, Andreas PASTOORS & Erich CLAßEN.....33-50
- Lithic assemblages from the Middle Paleolithic of Geißenklösterle Cave provide insights on Neanderthal behavior in the Swabian Jura**  
*Steinartefaktinventare aus dem Mittelpaläolithikum des Geißenklösterle, Deutschland: Neue Erkenntnisse zum Verhalten der Neandertaler auf der Schwäbischen Alb*  
 Nicholas J. CONARD, Viola C. SCHMID, Michael BOLUS & Manuel WILL.....51-80
- Everything lost? Reconstruction of Middle- and Upper Paleolithic occupations at the Felsenhäusl-Kellerhöhle, Lower Altmühl Valley (Franconian Jura, SE Germany)**  
*Alles verloren? Rekonstruktion mittel- und jungpaläolithischer Begehungen der Felsenhäusl-Kellerhöhle, Unteres Altmühltal (Fränkischer Jura, SO Deutschland)*  
 Merlin HATTERMANN, Alvise BARBIERI & Thorsten UTHMEIER.....81-110
- Geoarchaeology and geochronology of the Upper Palaeolithic site of Temerești Dealu Vinii, Banat, Romania: Site formation processes and human activity of an open-air locality**  
*Geoarchäologie und Geochronologie der jungpaläolithischen Fundstelle Temerești Dealu Vinii, Banat, Rumänien: Natürliche und menschliche Einflüsse auf die Genese einer Freilandfundstätte*  
 Wei CHU, Stephan PÖTTER, Adrian DOBOȘ, Thomas ALBERT, Nicole KLASSEN, Alexandru CIORNEI, Janina J. BÖSKEN & Philipp SCHULTE.....111-134
- A pre-Heinrich Event 3 assemblage at Fumane Cave and its contribution for understanding the beginning of the Gravettian in Italy**  
*Ein vor das Heinrich 3-Ereignis datierendes Inventar aus der Fumane-Höhle und sein Beitrag zum Verständnis des Beginns des Gravettien in Italien*  
 Armando FALCUCCI & Marco PERESANI.....135-154

<b>The Gravettian site Meča Dupka (Serbia) and its regional context</b> <i>Die Gravettien-Fundstelle Meča Dupka (Serbien) und ihr regionaler Kontext</i>	
<b>Senka PLAVŠIĆ &amp; Predrag POPOVIĆ.....</b>	<b>155-175</b>
<b>Pigments on Upper Palaeolithic mobile art. Spectral analysis of figurines from Mal'ta culture (Siberia)</b> <i>Pigmente auf jungpaläolithischer mobiler Kunst. Spektralanalyse von Statuetten der Mal'ta Kultur (Sibirien)</i>	
<b>Liudmila Valentinovna LBOVA.....</b>	<b>177-185</b>
<b>One ring to interpret. Bone ring-type adornment from the Epigravettian site Bratčice (Moravia, Czech Republic)</b> <i>Un anneau à interpréter. Un ornement en os de type anneau du site épigravettien de Bratčice (Moravie, République Tchèque)</i>	
<b>Zdeňka NERUDOVÁ , Bibiana HROMADOVÁ, Petr NERUDA &amp; František ZELENKA.....</b>	<b>187-200</b>
<b>Hassi Berkane and Late Iberomaurusian Land Use in the Eastern Rif, Morocco</b> <i>Hassi Berkane und die Landnutzung im späten Ibéromaurusien im östlichen Rif, Marokko</i>	
<b>Taylor OTTO, Helmut BRÜCKNER &amp; Gerd-Christian WENIGER.....</b>	<b>201-223</b>
<b>Kostënki 17 (Spitsynskaya) and Kostënki 6 (Streletskaya): recent fieldwork and new <sup>14</sup>C dates</b> <i>Kostënki 17 (Spitsynskaja) und Kostënki 6 (Streletskaja): jüngste Feldforschung und neue <sup>14</sup>C-Daten</i>	
<b>Rob DINNIS, Alexander BESSUDNOV, Alexei ARTYUSHENKO, Anton LADA, Andrei SINITSYN &amp; Thomas HIGHAM.....</b>	<b>225-230</b>
<b>Book reviews</b> <i>Buchbesprechungen.....</i>	<b>231-237</b>